

600 563

The Electrochemical Behavior of Armco Iron  
in Sulfuric Acid

TN-568

31 January 1964

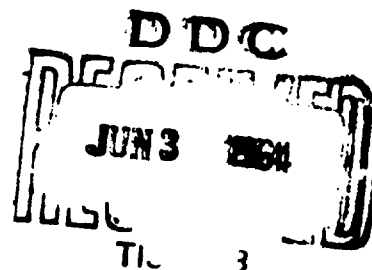
26-P-0.75

DDC AVAILABILITY NOTICE

Qualified requesters may obtain copies of  
this report from DDC.

U. S. NAVAL CIVIL ENGINEERING LABORATORY  
PORT HUENEME, CALIFORNIA

Best Available Copy



THE ELECTROCHEMICAL BEHAVIOR OF ARMCO IRON  
IN SULFURIC ACID

Y-R011-01-01-035

Type C

by

Howard A. Porte, Ph. D., Thomas E. Nappier

ABSTRACT

The polarization behavior of Armco iron in sulfuric acid solutions was investigated. Anodic and cathodic polarization curves were obtained using aerated and deaerated solutions of 1N and pH1 sulfuric acid by galvanostatic and potentiostatic methods.

## INTRODUCTION

Metallic corrosion is a serious problem with direct economic losses to the United States conservatively estimated to be about five and one half billion dollars annually;<sup>1</sup> consequently, much effort has been devoted to the development of methods for reducing or eliminating this problem. One of the more important fields of research in corrosion is the investigation of the passive phenomenon. The word passivity was first used by Schönbein<sup>2</sup> in 1836 to describe the peculiar inertness of iron immersed in concentrated nitric acid. Uhlig<sup>3</sup> has defined passivity as, "A metal active in the Emf Series, or an alloy composed of such metals, is considered passive when its electrochemical behavior becomes that of an appreciably less active or noble metal." In general, an active metal in an aggressive environment is described as "passive" when it is corrosion resistant, that is when it has a low corrosion rate.

It is now well established that the dissolution of metals in solution is an electrochemical process. Until recently, the study of metallic corrosion has been primarily empirical. Now, however, the introduction of modern electrochemical methods makes possible more fundamental corrosion studies. One of these methods, using polarization techniques, allows investigation of the corrosion rate of a metal in a solution over a wide range of electrode potentials. Electrochemical polarization curves may be obtained in two ways, depending on the choice of the independent variable.

Potentiostatic polarization refers to measurements when the potential is the independent variable and the resultant current is observed and recorded. Potentiostatic polarization curves are obtained by using a device called the potentiostat which automatically adjusts the polarizing current (dependent variable) to whatever value is required to maintain the prevailing potential. Experimentally, such curves are obtained by an arbitrary technique and usually each investigator adheres to a particular method. In one method polarization curves are obtained point-by-point, using a truly "potentiostatic" technique. The current, which is time dependent, is measured at a fixed potential, after either an arbitrarily fixed time interval or after a steady-state has been reached, sometimes after several hours.<sup>4</sup> Another method (now often called the "potentiodynamic" method) is to measure current continuously while the voltage setting of the potentiostat is changed at a constant rate by an electric motor.<sup>5</sup>

It was recognized at an early stage that different techniques would give polarization curves differing in detail<sup>5</sup> and a recent study<sup>6</sup> described some effects of variations in technique on polarization curves obtained with a potentiostat.

When the current is the independent variable, it is called galvanostatic polarization. Galvanostatic polarization curves are obtained by employing a circuit in which the current is maintained constant and the potential is allowed to vary at will.

With potentiostatic anodic polarization, Figure 1, a metal such as iron reaches a maximum current density; then as the potential is raised to more noble values, the current density drops to a very low value indicating a low rate of metal dissolution. This area of low corrosion rate is the passive region; the transpassive region is reached upon raising the potential further and oxygen evolution is observed with increasing current density. The passive region is not observed with galvanostatic polarization, Figure 2, instead a shift in potential over this region takes place.

Fundamental to corrosion studies are anodic and cathodic polarization measurements to determine the corrosion potential and corrosion current in different environments. The basic principles for the use of polarization measurements have been well developed through the theory of mixed potentials.<sup>7</sup> Stern and Geary<sup>8</sup> have shown that in corroding systems controlled by activation polarization, i.e., where the local anodic and cathodic polarization curves are logarithmic, the following relation applies:

$$\frac{\Delta E}{\Delta I} = \frac{\beta_a \beta_c}{2.3(I_{\text{corr}}) (\beta_a + \beta_c)}$$

where  $\frac{\Delta E}{\Delta I}$  is the polarization resistance,  $\beta_a$  and  $\beta_c$  are the Tafel slopes of the logarithmic local anodic and cathodic curves, Figure 3, and  $I_{\text{corr}}$  is the corrosion current. It is important to note that this equation only applies when the change in potential,  $\Delta E$ , from the corrosion potential is very small, being of the order of a few millivolts.

For a corroding electrode controlled by concentration polarization, i.e., when the reaction rate or applied current is so large that the reacting species cannot reach the electrode at a sufficiently rapid rate, the following equation has been found to hold:

$$\frac{\Delta E}{\Delta I} = \frac{-\beta_a}{2.3(I_{\text{corr}})}$$

Therefore, whether a corroding electrode is controlled by activation or concentration polarization, it will still produce, in the vicinity of the corrosion potential, a linear polarization curve the slope of which is inversely related to the corrosion current. Thus, the corrosion rate may be calculated for a given system if the  $\beta$  values and the polarization resistance are known. The  $\beta$  values are determined from the logarithmic polarization curves, Figure 3; however, if the polarization curves are not experimentally determinable the  $\beta$  values may be estimated since the large majority lie within a narrow range. The polarization resistance may be determined from linear plots of voltage versus applied current, Figure 4.

The derivation of Stern implies equal slopes  $\left(\frac{\Delta E}{\Delta I}\right)$  for both anodic and cathodic polarization; however, this is not always the case. Therefore, in practice only one polarization curve (cathodic) is used to evaluate the polarization resistance and subsequently the corrosion current ( $I_{\text{corr}}$ ).

#### EXPERIMENTAL

The apparatus in the galvanostatic polarization investigations, Figure 5, was similar to that of Nobe and Tobias.<sup>6</sup> The cell was a 3-liter or a 12-liter vessel covered with Lucite top, Figure 6, with appropriately placed portholes. The electrode assembly, Figure 7, was constructed such that a mercury seal cup for electrical contact held the center rotating electrode at minimal eccentric motion through a Teflon bearing. Teflon sleeves were used to isolate the stainless rod from the solution and Tygon gaskets were used as seals to prevent leakage at joints.

In order to minimize IR drops across the solution a capillary probe was connected to the calomel electrode reservoir; the solution was drawn into the reservoir by an aspirator and retained electrical conductivity through a greaseless stopcock. The platinum counter electrode was isolated from the main solution by a fritted glass disk and a fritted glass bubbler was used to introduce the test gases.

The potential versus saturated calomel electrode (S.C.E.) was measured with a high input impedance Keithley Model 603 Electrometer Amplifier with 2% of full scale accuracy on all scales and a zero drift of less than 2 millivolts per hour, the output being recorded on a Varian Model G-10 recorder, or alternatively determined using a Leeds and Northrop K-2 potentiometer with a Type E galvanometer. The current was measured with a Hewlett-Packard Model 412A vacuum tube voltmeter (VTVM) with 2% of full scale accuracy on all scales. For the power supply two banks of three 45V batteries in series and several variable resistors up to about four megohms provided substantially stable current at about 135 volts. The iron electrode was rotated at 160 rpm by a Universal Bodine motor controlled by a variable transformer and a stroboscope was used to check its speed. The purpose of the rotation was to reduce concentration polarization effects.

Potentiostatic measurements, Figure 8, were obtained by the use of a Wenking 61-TR potentiostat using the built-in ammeter or the same VTVM as used previously to measure the current.

#### PROCEDURE

The iron electrodes were fabricated from one-half inch Armco iron rod of the following manufacturers analysis:

C	-	.020%	S	-	.018
Mn	-	.044	Si	-	.004
P	-	.003	Cu	-	.092
			Fe	-	Balance

The rod was machined into cylinders with thicknesses of one-half inch and one-fourth inch corresponding to curved surface areas of 5 cm<sup>2</sup> and 2.5 cm<sup>2</sup>. The centers were drilled and tapped so that they could be threaded on one-fourth inch stainless steel rod. The electrodes were polished with No. 280 and No. 400 emery paper in that order; after assembling the electrode, Figure 7, the exposed surface was degreased with acetone, chloroform and carbon tetrachloride, then activated in 3:1 HNO<sub>3</sub> for five minutes and 5N H<sub>2</sub>SO<sub>4</sub> for fifteen minutes until the attack appeared uniform as observed by hydrogen evolution. Upon rinsing the exposed areas thoroughly with demineralized water, the electrode assembly was installed in the cell and a steady-state open circuit Emf was measured as soon as possible. In galvanostatic experiments, the current from the power supply was increased at regular time intervals varying from two to five minutes or until an apparent steady-state potential was observed on the recorder chart.

The solutions were diluted from Analytical Reagent grade concentrated H<sub>2</sub>SO<sub>4</sub> and pH 1 solutions were checked with a Beckman Model G pH meter. The solutions were aerated at least one hour or were deaerated for at least sixteen hours with nitrogen before installing the electrode assembly; the air or nitrogen flow was continued throughout the experiment. In both cases the gases were bubbled through demineralized water before reaching the solution. The temperature of the solution was 26 ± 1°C during the experiments.

Potentiostatic measurements were made in much the same way as galvanostatic experiments and in both methods the iron electrode was grounded using the electrometer single-ended.

## RESULTS AND DISCUSSION

Polarization measurements at first would seem to be quite uncomplicated and straightforward; however, these investigations demonstrate the fact that a large number of variables must be controlled to get reproducible results.

A measurement which was difficult to obtain was the steady-state open circuit Emf. It was found that the electrode may take from one hour to several hours to come to an equilibrium steady-state after being installed into the system and also that after being polarized the electrode may take several hours to reach steady-state open circuit equilibrium

again. Upon interrupting the current, i.e., opening the circuit after polarizing anodically, the potential dropped below the open circuit value, then rose again, Figure 9, approaching the open circuit steady-state value.

The corrosion potential of iron measured in deaerated solutions was very nearly the same as in aerated solutions, but the measurements were far more difficult to reproduce in aerated solutions.

In all instances, the steady-state potentials were influenced by the rotation rate of the electrode, which was held as constant as possible, nevertheless varied a few rpm and thus very probably caused a variation of the potential field around the electrode. The eccentric motion of the electrode during rotation, in which the distance to the tip of the capillary probe would vary slightly, was considered to be only a minor cause for potential oscillation. The use of the capillary probe reduced the IR drop to an essentially negligible correction. The rotation of the electrode reduced concentration polarization and dispersed the hydrogen formed upon cathodic polarization as well as the oxygen formed in the transpassive region. During galvanostatic polarization the Emf consistently oscillated to the extent of  $\pm 1$  mv while the electrode was turning; however, at the higher current densities, viz.  $0.5 \text{ ma/cm}^2$ , this oscillation often dropped to  $\pm 0.5$  mv or less. Large gas flows bubbling through the solution during a polarization run caused very large erratic oscillations ( $\pm 5$  mv) in the potential; when the bubbling was reduced to a minimum, this erratic oscillation disappeared and a steady, low-amplitude oscillation ( $\pm 1$  mv) was observed on the recorder chart.

Cathodic polarization yielded the most consistent results in obtaining continuous curves; whereas, anodic curves were difficult to obtain and often showed unexplainable breaks. The time dependence of the anodic curve was well illustrated by the strip chart recording the Emf after changing the current, Figure 10; at higher anodic currents, viz.  $1 \text{ ma/cm}^2$ , the time to reach a steady state potential was often up to twenty minutes. The shift in corrosion potential  $E_{\text{corr}}$ , in changing from pH 1 to 1N (pH 0.2) solutions was in the noble direction,  $E_{\text{corr}}$  being  $-0.040$  volts. Hysteresis was exhibited in both curves, the effect being a displacement of the curve closer toward the open circuit Emf value.

Typical galvanostatic polarization curves obtained in this investigation are illustrated in Figures 11 to 13. The results are summarized in Tables 1 and 2. On the basis of the "polarization resistance" equation derived by Stern, these data would predict that the rate of corrosion of iron in sulfuric acid solution would show the following relationships: 1N aerated > 1N deaerated > pH1 deaerated, i.e., the corrosion rate of iron should increase in the presence of dissolved oxygen and decrease with increasing pH. These are in fact the same effects reported<sup>7,8</sup> for the corrosion behavior of iron.

TABLE 1. Polarization Data

H <sub>2</sub> SO <sub>4</sub> Solution	Linear Slope (ohm-cm <sup>2</sup> )		Tafel Slope (volts)		Corrosion Potential vs S.C.E. (mv)
	Anodic	Cathodic	Anodic	Cathodic	
pH 1 Deaerated	167	200	0.048	0.102	-502
1N Deaerated	124	144	0.036	0.092	-472
1N Aerated	82	98	0.035	0.120	-473

TABLE 2.

## Galvanostatic Polarization of Armco Iron in Sulfuric Acid

Applied Current (mA/cm <sup>2</sup> )	Potential Versus Saturated Calomel Electrode (mv)					
	IN H <sub>2</sub> SO <sub>4</sub> , Deaerated		IN H <sub>2</sub> SO <sub>4</sub> , Aerated		pH 1 H <sub>2</sub> SO <sub>4</sub> , Deaerated	
	Anodic	Cathodic	Anodic	Cathodic	Anodic	Cathodic
0.010	-471	-472	-472	-481	-502	-498
0.020	-469	-474	-471	-482	-501	-500
0.030	-468	-475	-470	-483	-499	-501
0.040	-467	-476	-469	-484	-497	-503
0.050	-466	-477	-468	-485	-496	-505
0.060	-464	-479	-467	-486	-494	-506
0.090	-462	-482	-465	-490		-510
0.100	-461	-483	-464	-491	-486	
0.180	-456	-493	-460	-500		-522
0.200	-454	-496	-460	-503	-473	
0.280	-451	-505	-457	-513		-534
0.300		-507	-457	-516	-465	
0.400	-445	-518	-455	-526		-546
0.480	-443	-525	-451	-531		-553
0.500					-450	
0.580						-561
0.600	-442	-535	-448	-547		
0.700						-567
0.800		-546	-444	-562	-439	-574
0.860	-442					
0.900		-552	-441	-568		-579
0.960	-441					
1.00		-556	-437	-575		-583
1.30	-437					-595
1.40		-572		-598	-412	
1.50	-435					
2.00	-429	-591		-623	-380	-614
2.80	-418	-609		-649		
3.00					-334	-634
3.40		-622		-667		
4.00	-404	-633		-685		
4.20						-653
4.60		-643		-701		
5.00						-662
5.80	-383					
6.00						-676
6.40		-673				
7.00						-687
8.00						-698
8.40	-354					

Blank spaces indicates that no reading was taken.

The linear slopes and Tafel slopes denoted in Table 1 are those obtained initially after the electrode was inserted in the solution; it was noticed that these slopes decreased up to 50% upon "aging" of the electrode and solution for a period of about a week. During this aging process a light colored ring formed on the electrode in the same horizontal plane as the capillary probe; this ring, indicating some type of film, presumably affected the polarization measurements. In this period the surface of the electrode became severely etched and deeply pitted with noticeably uneven corrosion especially near the edges, whereas the electrodes removed immediately after the potentiostatic runs were quite smooth, showing uniform dissolution. In all of the cathodic curves, there was a definite continuous curvature and no completely straight-line function was obtainable, although an area of apparent beginning linearity appeared. These regions of near linearity were obtained only when the current was changed a comparatively small amount from the previous setting.

In the investigation of the phenomena of passivity it was observed that the return path of the galvanostatic anodic polarization, was quite similar to that of potentiostatic polarization. By using a constant current power supply in the iron-platinum circuit, it was possible to enter the passive region from the transpassive region, but this proved to be a poor control device as the Emf shifted about 800 mv at the active-passive transition area; only a 40 mv shift in the same transition region was observed when the Wenking potentiostat was employed. In the active region near the transition area, the current as well as the potential varied greatly; these seemingly unstable conditions are probably due to the beginning formation of the passive film.

Typical potentiostatic polarization curves are illustrated in Figures 14 and 15 and the data are summarized in Table 3.

During potentiostatic polarization a black film built up on the surface of the electrode while in the active region; however, upon entering the passive region the film flaked off, fell to the bottom of the cell, and left a shiny metallic surface on the electrode. Again, hysteresis was exhibited in the passive region, the descending current densities in the passive region being much lower than the corresponding ascending values. The critical current density in both the aerated and deaerated 1N solutions was about 350 ma/cm<sup>2</sup>; however, the value was slightly larger in the aerated solution.

TABLE 3.

## Potentiostatic Polarization of Armco Iron in Sulfuric Acid

Potential vs. SCE. (mv)	Current Density (ma/cm <sup>2</sup> )			
	IN H <sub>2</sub> SO <sub>4</sub> , Aerated Ascending Descending		IN H <sub>2</sub> SO <sub>4</sub> , Deaerated Ascending Descending	
-475		2.1		0.64
-460	0.16			
-450	0.40	2.5	0.86	1.8
-400	14.	13.	17.5	16.1
-360	27			
-350				37
-300	48	52	64	64
-250	68			
-200	88	96	127	128
-100	136	148	193	192
0	188	196	256	237
+100	244	236	305	242
200	296	272	250	256
300	340	316	*	283
350	*	*	*	0.33
375	*	*	*	0.28
400	228*	0.012*	*	0.13
450	210*		*	
500	395*	0.015	0.033	0.018
600	395*	0.019	0.033	0.021
700	395	0.022	0.036	0.023
800	0.08	0.025	0.040	0.024
900	0.08	0.026	0.042	0.026
1000	0.08	0.031	0.046	0.028
1100	0.08	0.037	0.051	0.032
1200	0.08	0.056	0.064	0.050
1300	0.24	0.20	0.13	0.16
1400	0.68	0.68	0.25	0.25
1500	0.80	0.84	0.30	0.33
1600	1.7	1.5	3.95	7.3
1700	19	20	44.7	50
1800	60	60	106	108
1900	104	104	171	171
2000	140	140		

\* UNSTEADY

Blank space indicates that no reading was taken.

## CONCLUSIONS

The corrosion potential of iron in sulfuric acid solutions was dependent on the pH, shifting to more noble values, i.e., increasing, with decreasing pH. The "polarization resistance" technique indicated qualitatively that the corrosion rate should be greater in aerated than deaerated solutions and should increase with decreasing pH. The Tafel slopes were determined to be about 0.04 volts for anodic polarization and 0.1 volts for cathodic polarization of iron in aerated and deaerated 1N H<sub>2</sub>SO<sub>4</sub>.

Potentiostatic polarization exhibited typical S-shaped curves with a critical current density of 350 ma/cm<sup>2</sup>. Hysteresis loops were observed for ascending and descending sets of curves, the descending current densities being lower than the corresponding ascending values.

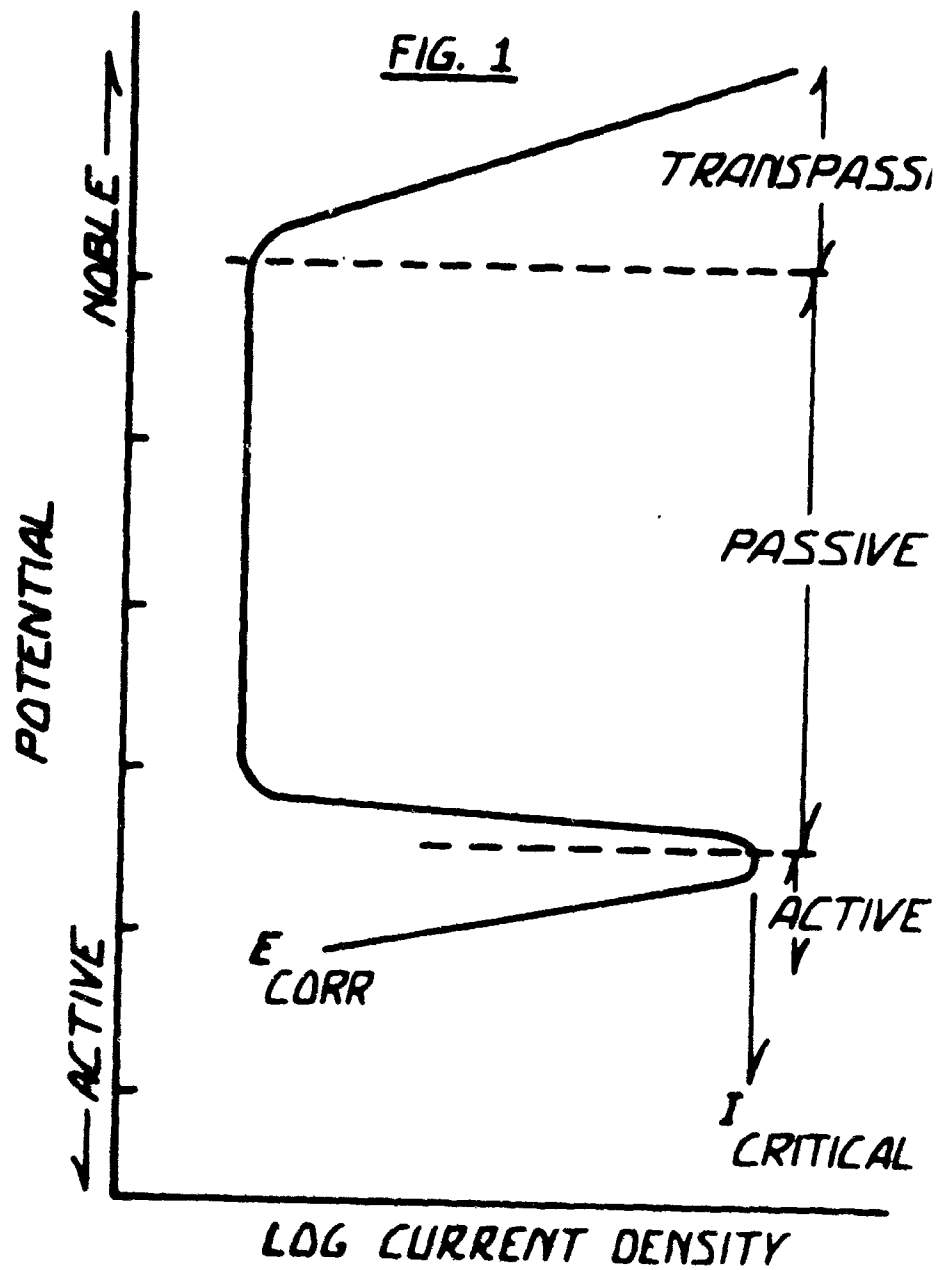
## FUTURE WORK

This report is the first in a series which will deal with the investigations of the electrochemical characteristics of various electrode-electrolyte systems. The long range objective of these investigations is the elucidation of the mechanisms of the electrochemical and physical transformations that occur at electrode-electrolyte interfaces. Intimate knowledge of the details of these transformations is of vital importance in the prevention and control of corrosion.

## REFERENCES

1. H. H. Uhlig. "Corrosion and Corrosion Control". John Wiley and Sons, Inc., New York, 1963, p. 3.
2. C. Schönbein, Pogg. Ann. 37, 590 (1836).
3. H. H. Uhlig, "The Corrosion Handbook," John Wiley and Sons, Inc., New York, 1948. p. 21.
4. N. D. Greene, "First International Congress on Metallic Corrosion," Butterworths, London, 1962. p. 113.
5. C. Edleanu, J. Iron St. Inst., 193, 360 (1959)

6. R. Littlewood, Corrosion Sci., 3, 99 (1963).
7. C. Wagner and W. Traud. Z. Electrochem., 44, 391 (1938)
8. M. Stern and A. L. Geary. "Electrochemical Polarisation I. A Theoretical Analysis of the Shape of Polarization Curves." J. Electrochem. Soc., 104, 56 (1957). M. Stern. "A Method for Determining Corrosion Rates from Linear Polarization Data". Corrosion, 14, 440t (1958).
9. K. Mabe and R. J. Tobias. "Aqueous Oxygen Corrosion of Armco Iron. Effect of Chloride Ions on Potentiostatic Phenomena in  $H_2SO_4$ ." Department of Engineering, University of California, Los Angeles, Report No. 63-11, (1963).
10. W. Whitman and R. Russell, Ind. and Eng. Chem., 17, 348 (1925).
11. K. J. Vetter. Z. Electrochem., 59, 67 (1955).



POTENTIOSTATIC  
ANODIC POLARIZATION  
(SCHEMATIC)

FIG. 2

SIVE

O<sub>2</sub> EVOLUTION

V

POTENTIAL

E

ACTIVE

LOG CURRENT DENSITY

GALVANOSTATIC  
ANODIC POLARIZATION  
(SCHEMATIC)

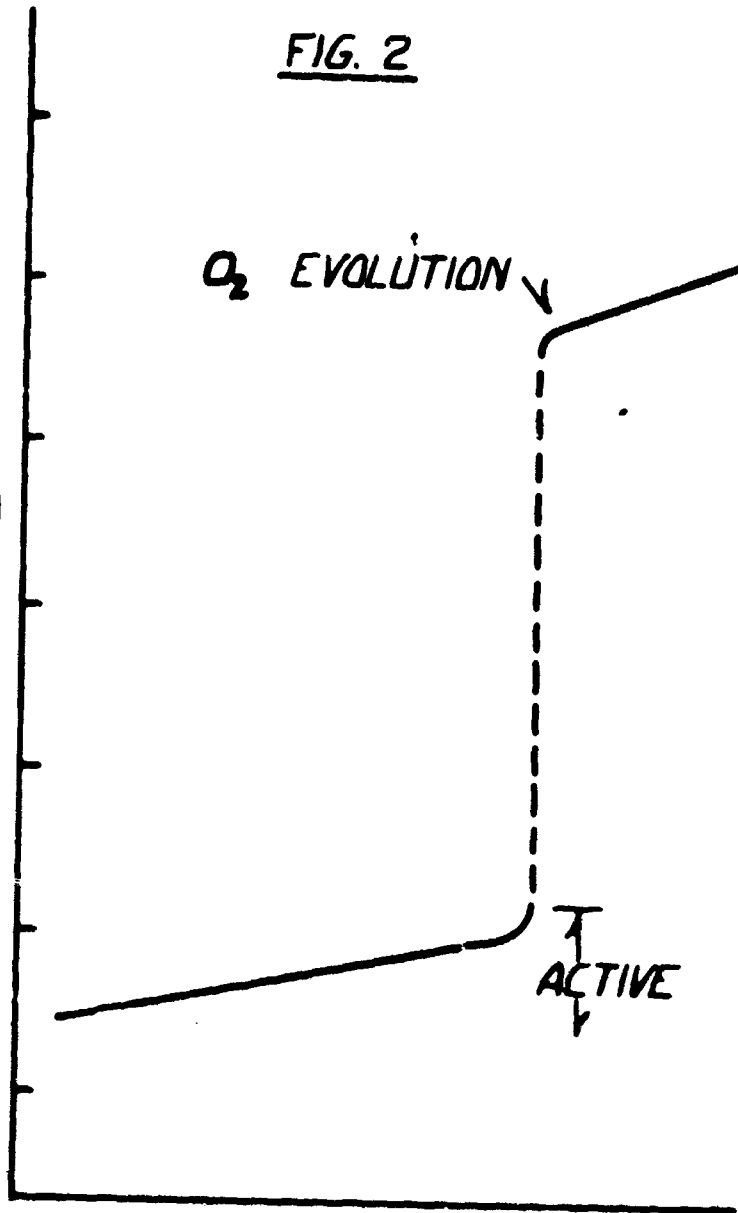
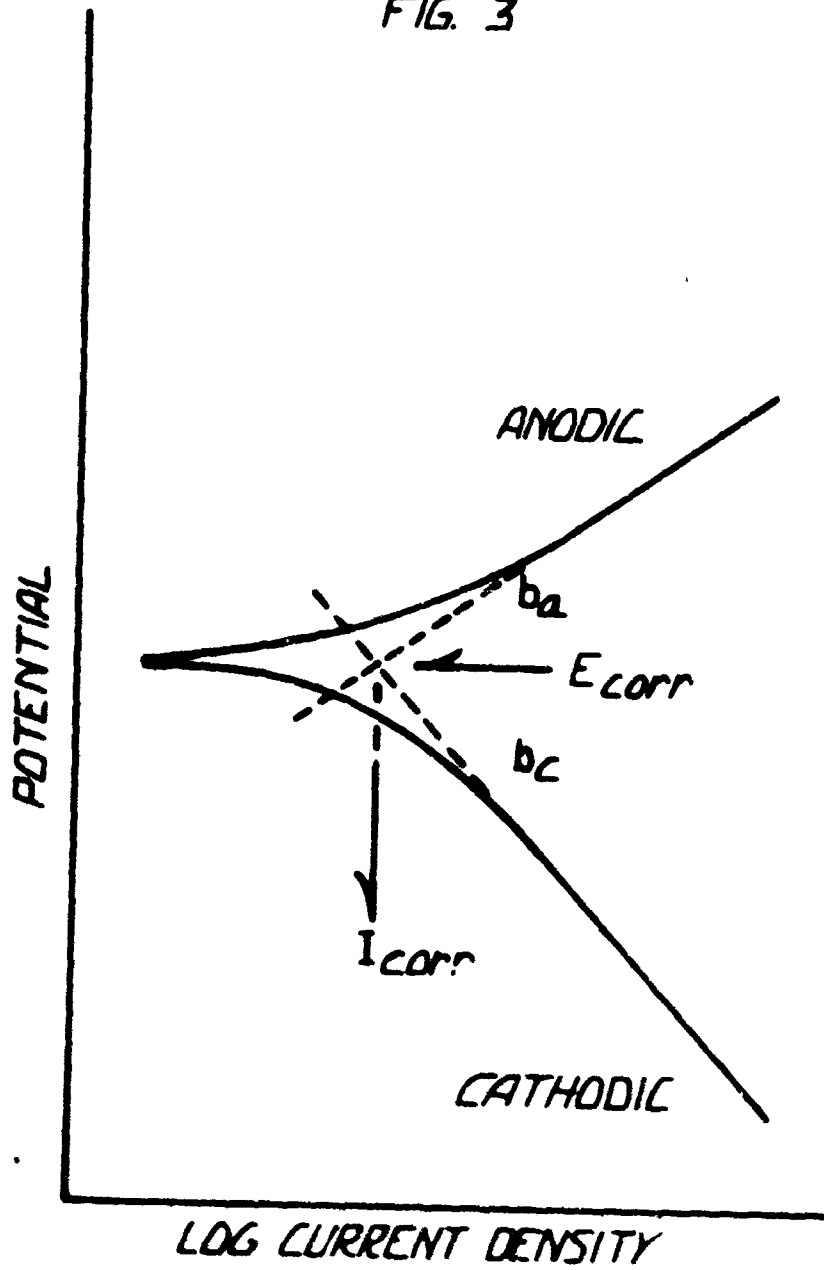
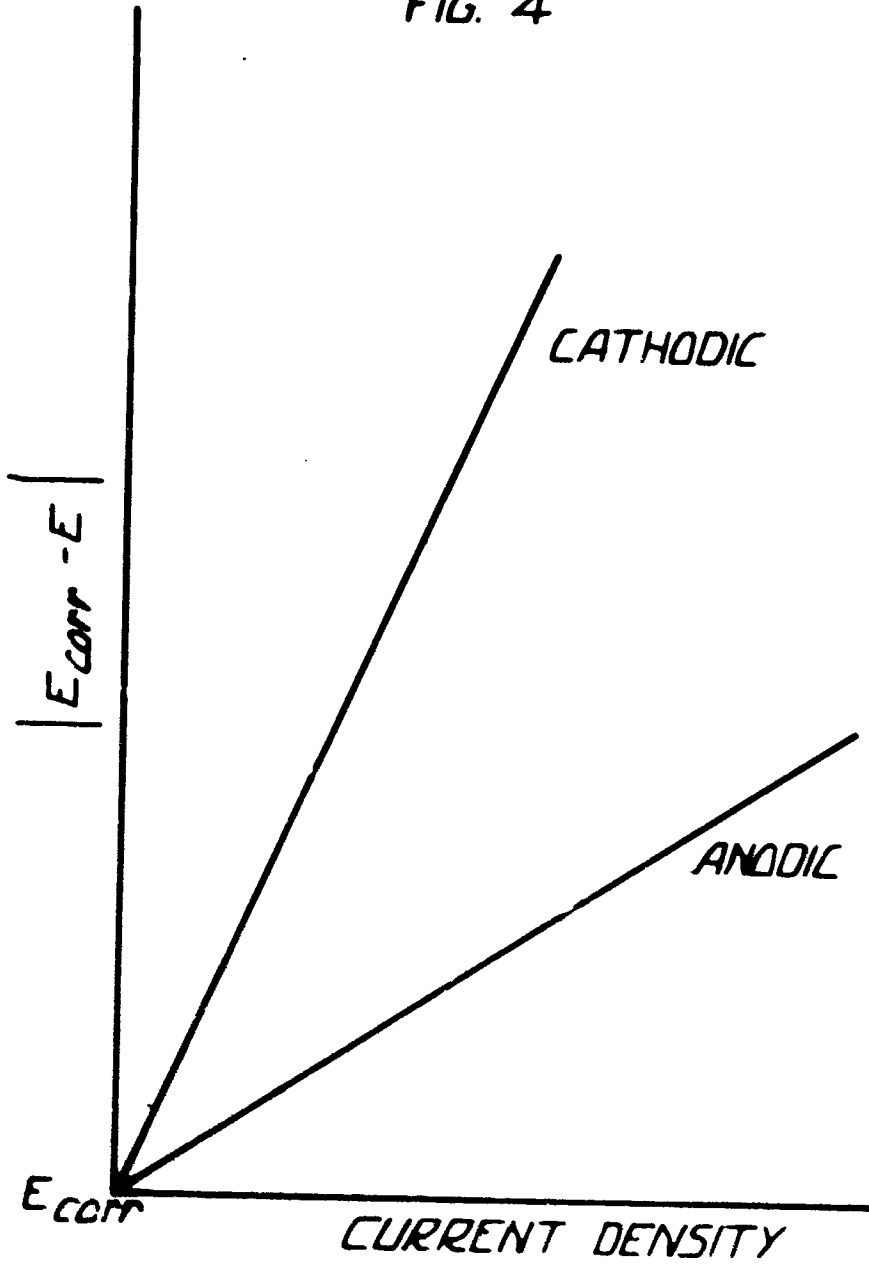


FIG. 3



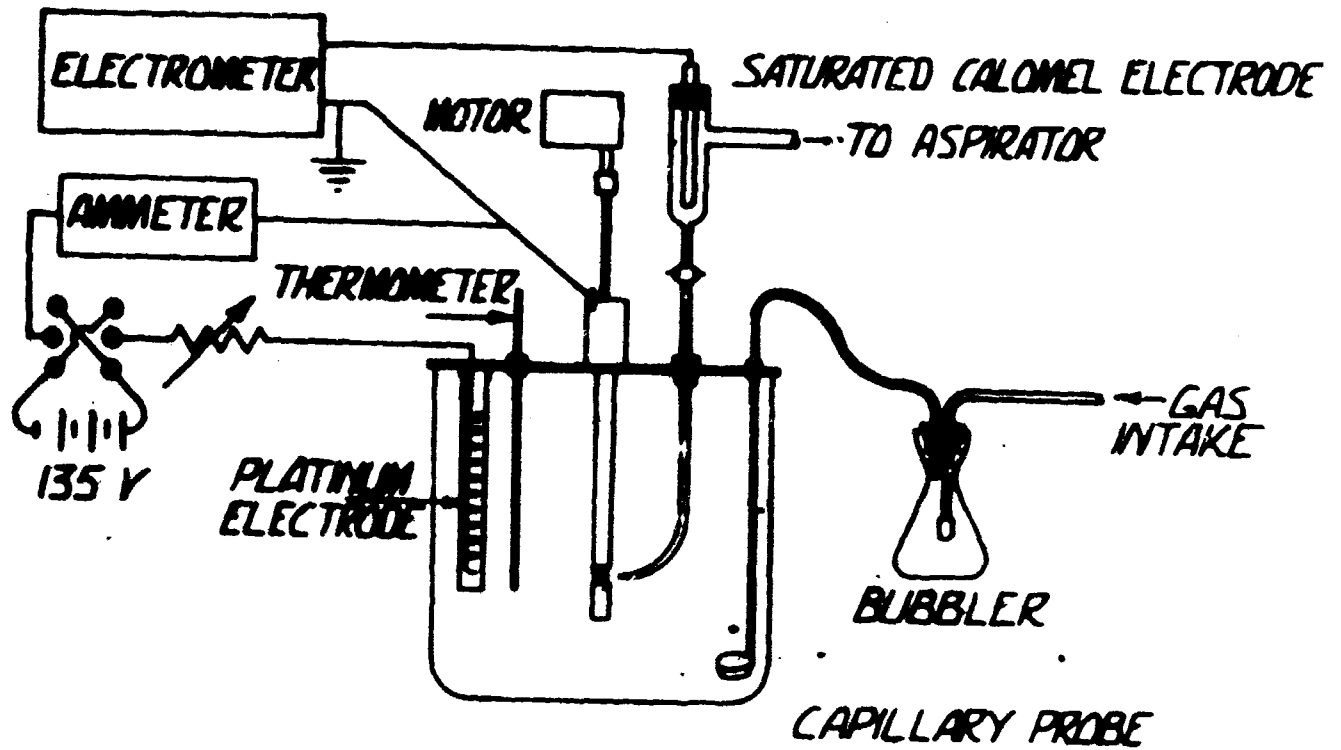
GALVANOSTATIC  
POLARIZATION CURVES  
(SCHEMATIC)

FIG. 4



LINEAR  
POLARIZATION CURVES  
(SCHEMATIC)

FIG. 5



GALVANOSTATIC POLARIZATION APPARATUS

FIG. 6

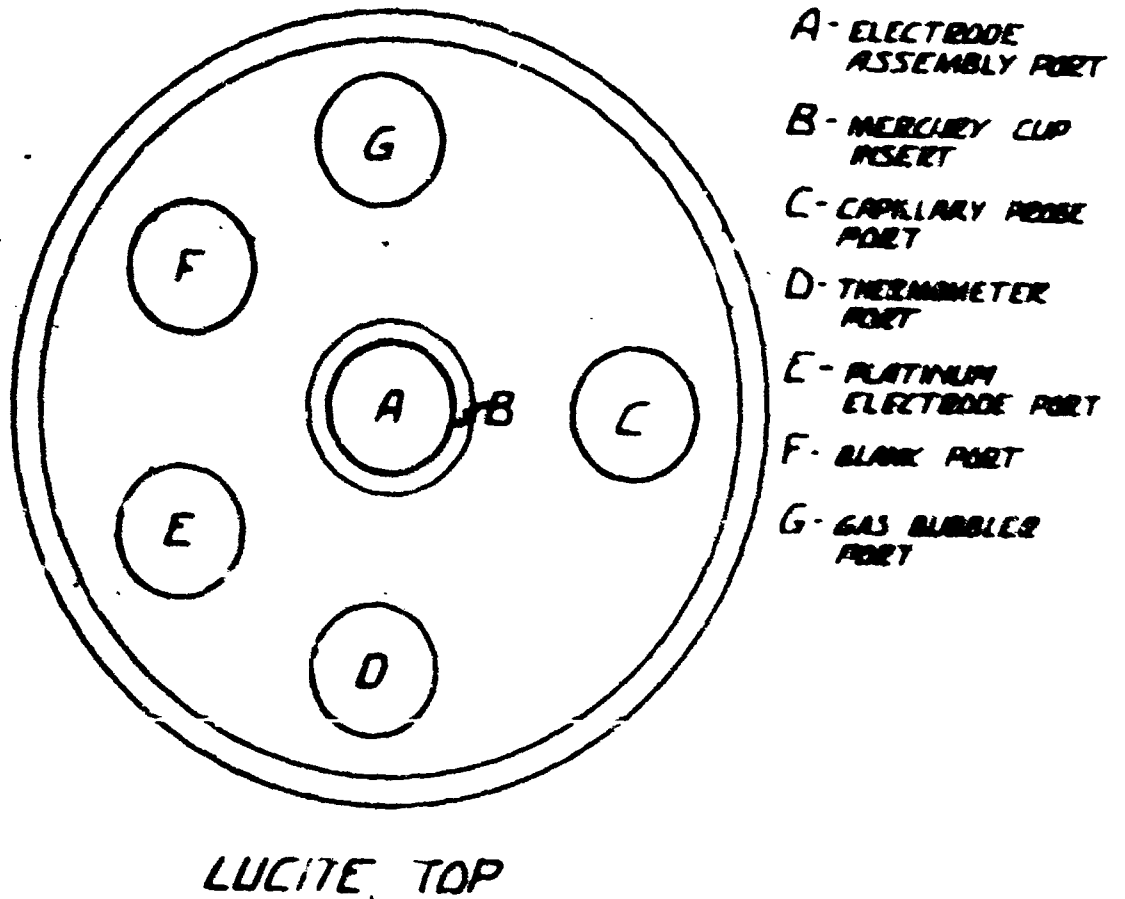


FIG. 7

$\frac{1}{4}$ " STAINLESS STEEL ROD

STAINLESS STEEL CUP

$\frac{1}{2}$ " TEFLON TUBING

TYGON GASKET

$\frac{1}{2}$ " TEST ELECTRODE

TEFLON TIP

TEST ELECTRODE  
ASSEMBLY

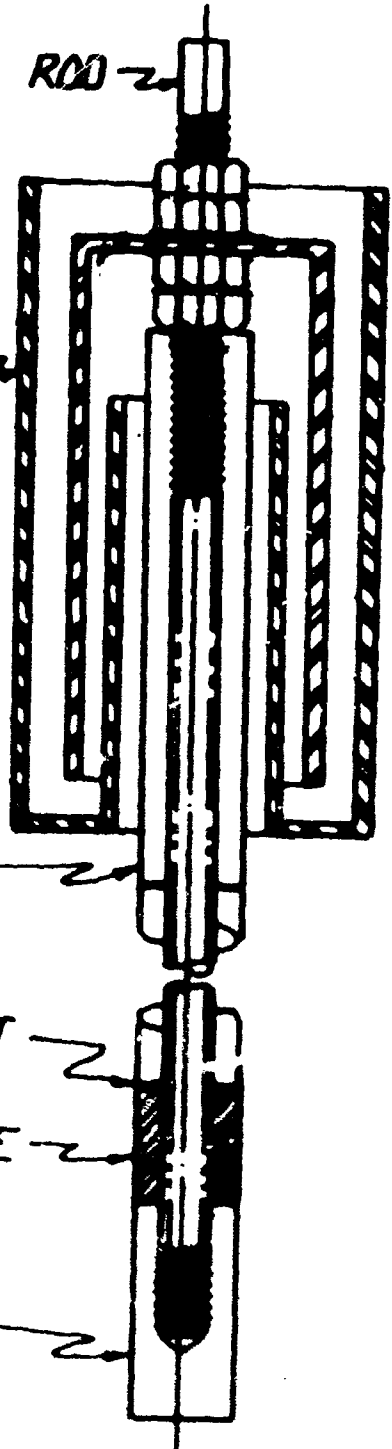
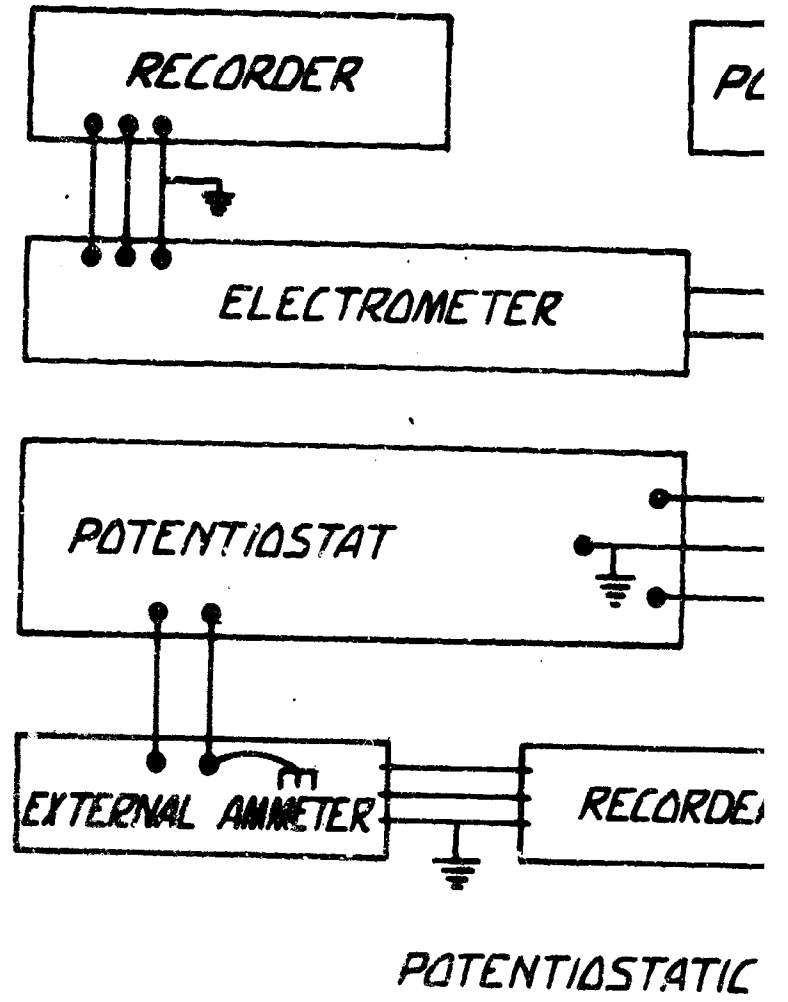
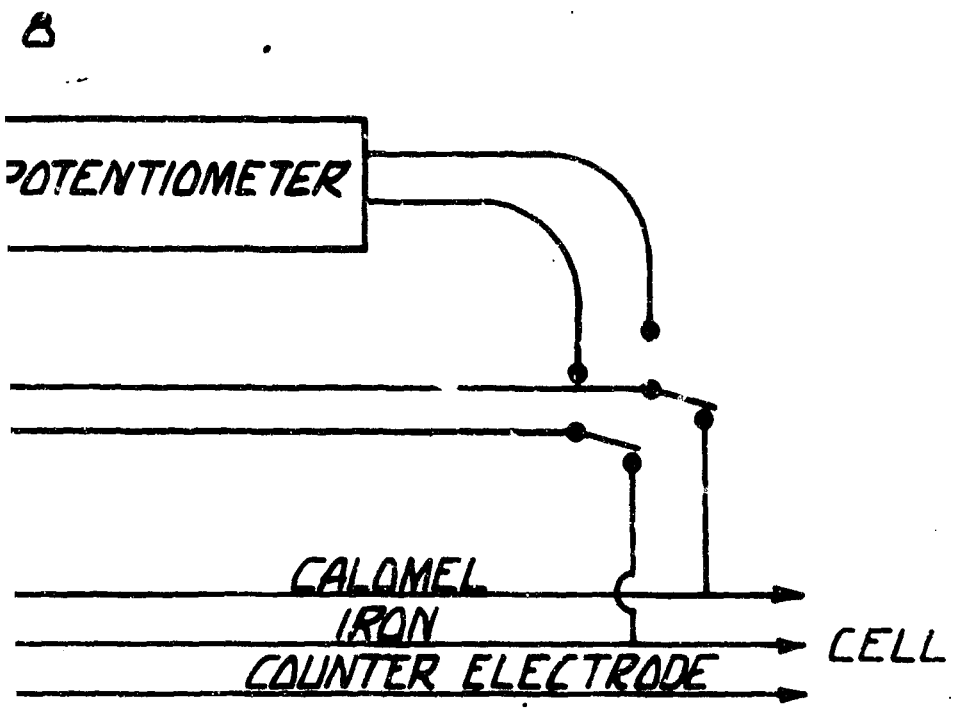


FIG. 6

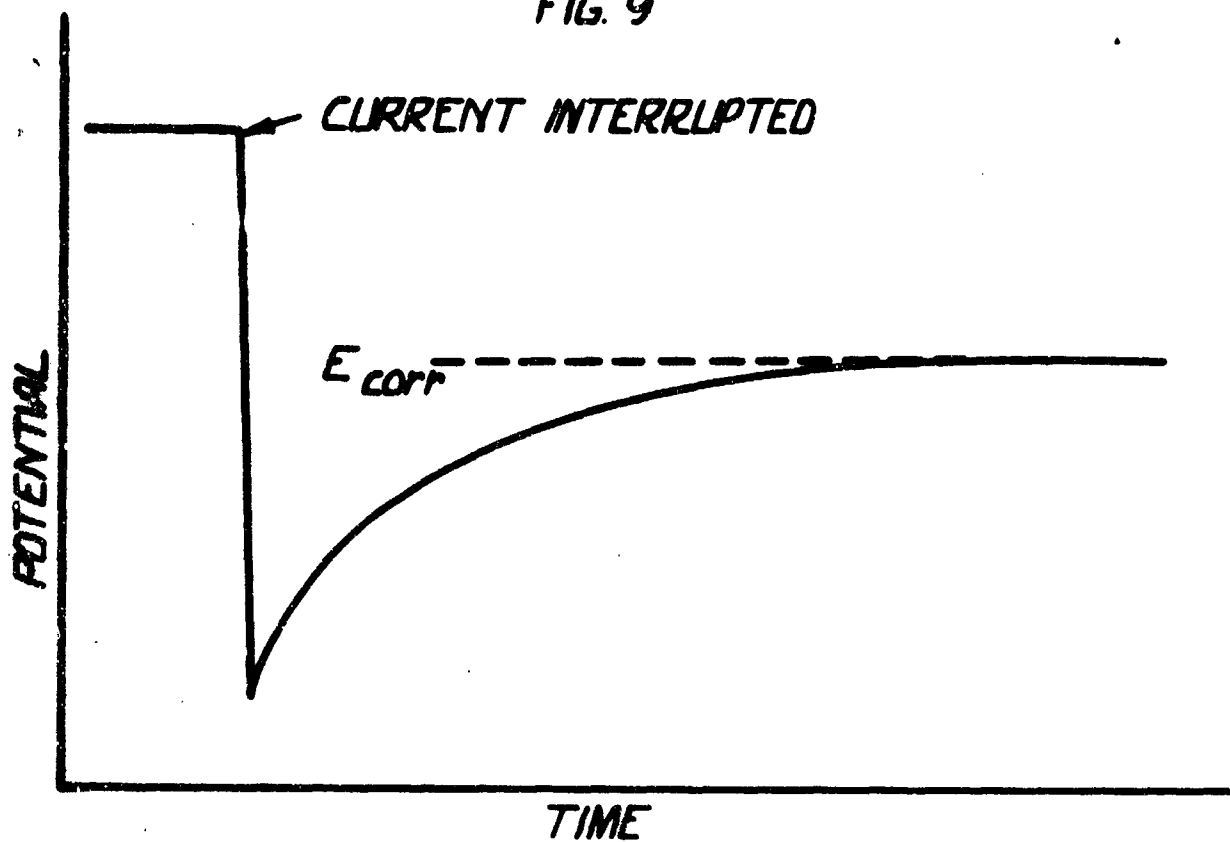




ER

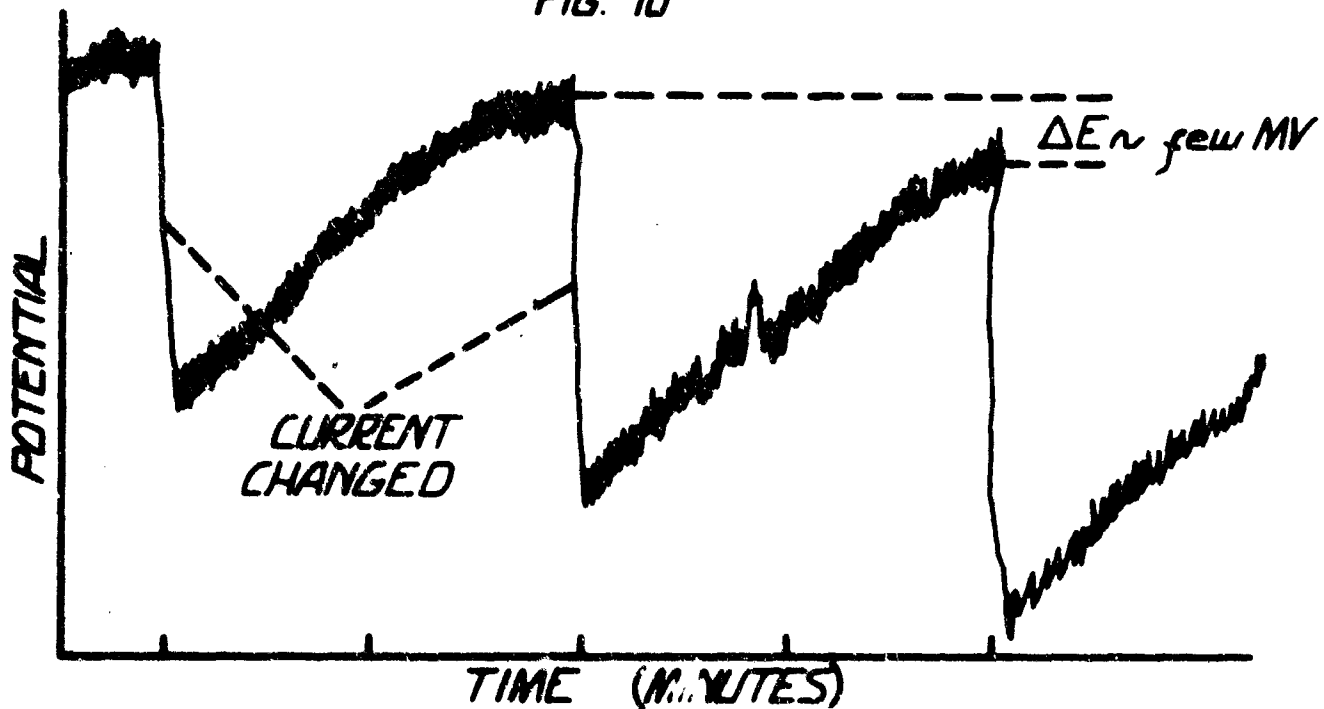
C POLARIZATION SET-UP

FIG. 9



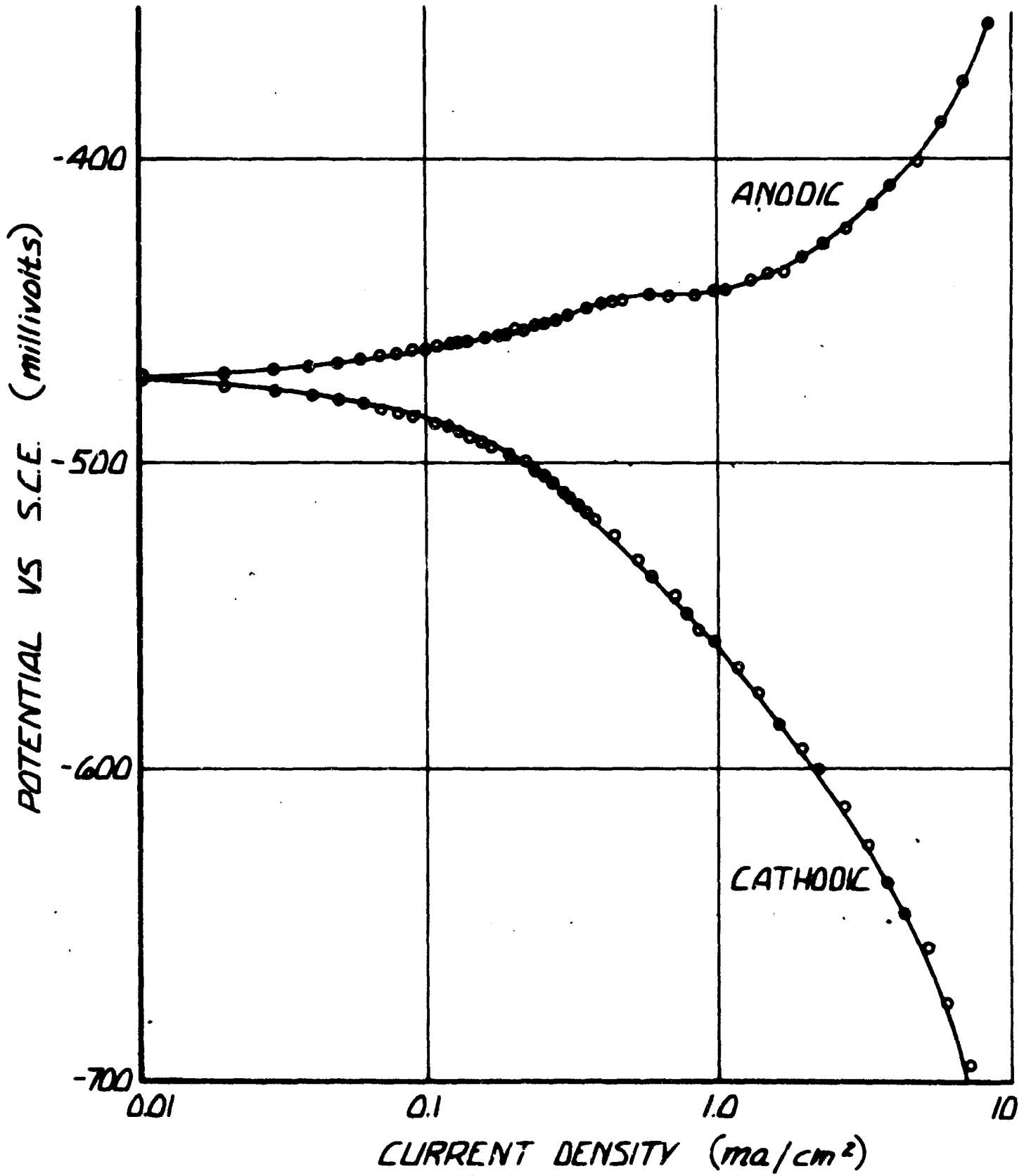
TIME-POTENTIAL DEPENDENCE UPON CURRENT INTERRUPTION

FIG. 10



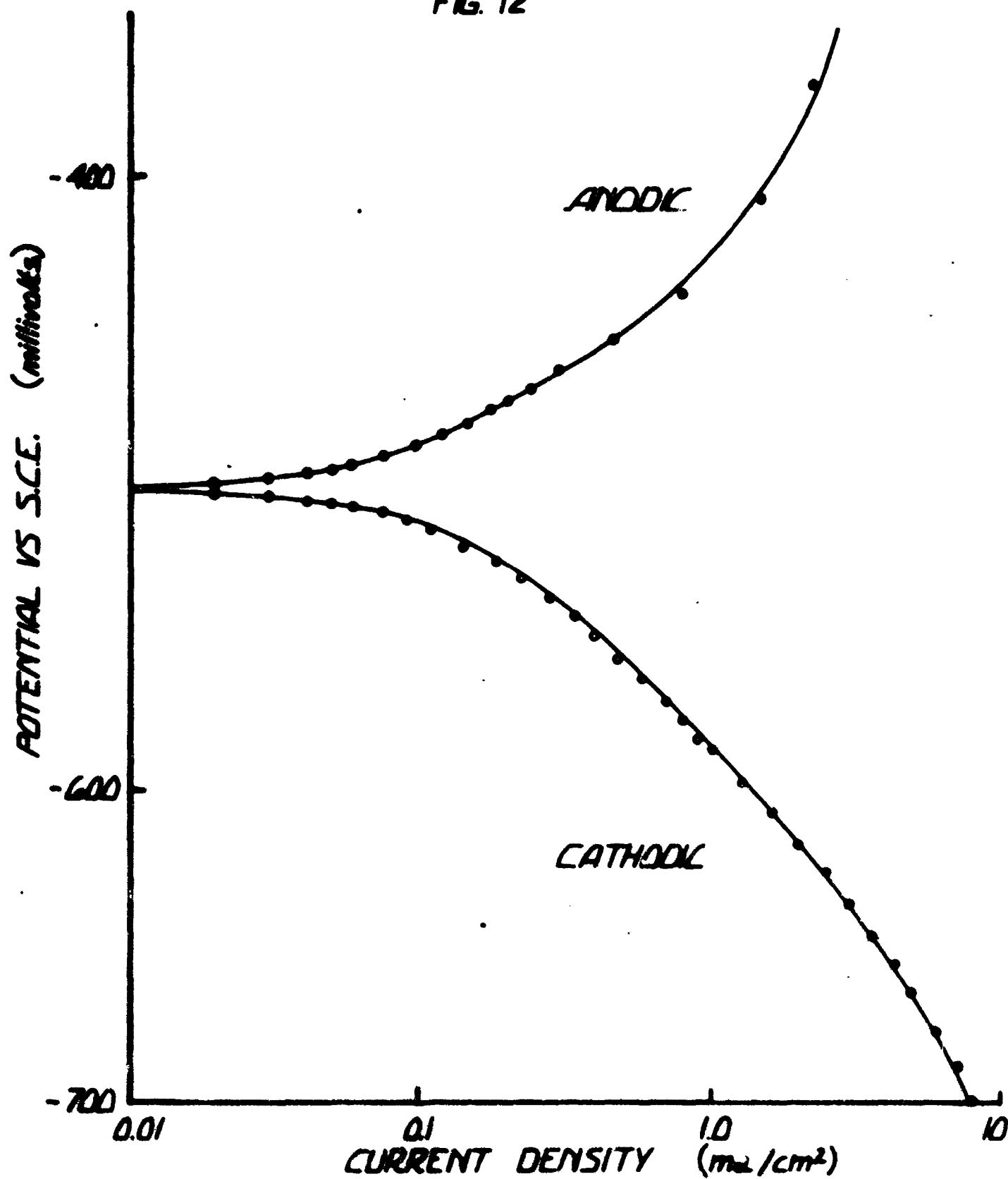
STRIP CHART RECORDER DATA

FIG. 11



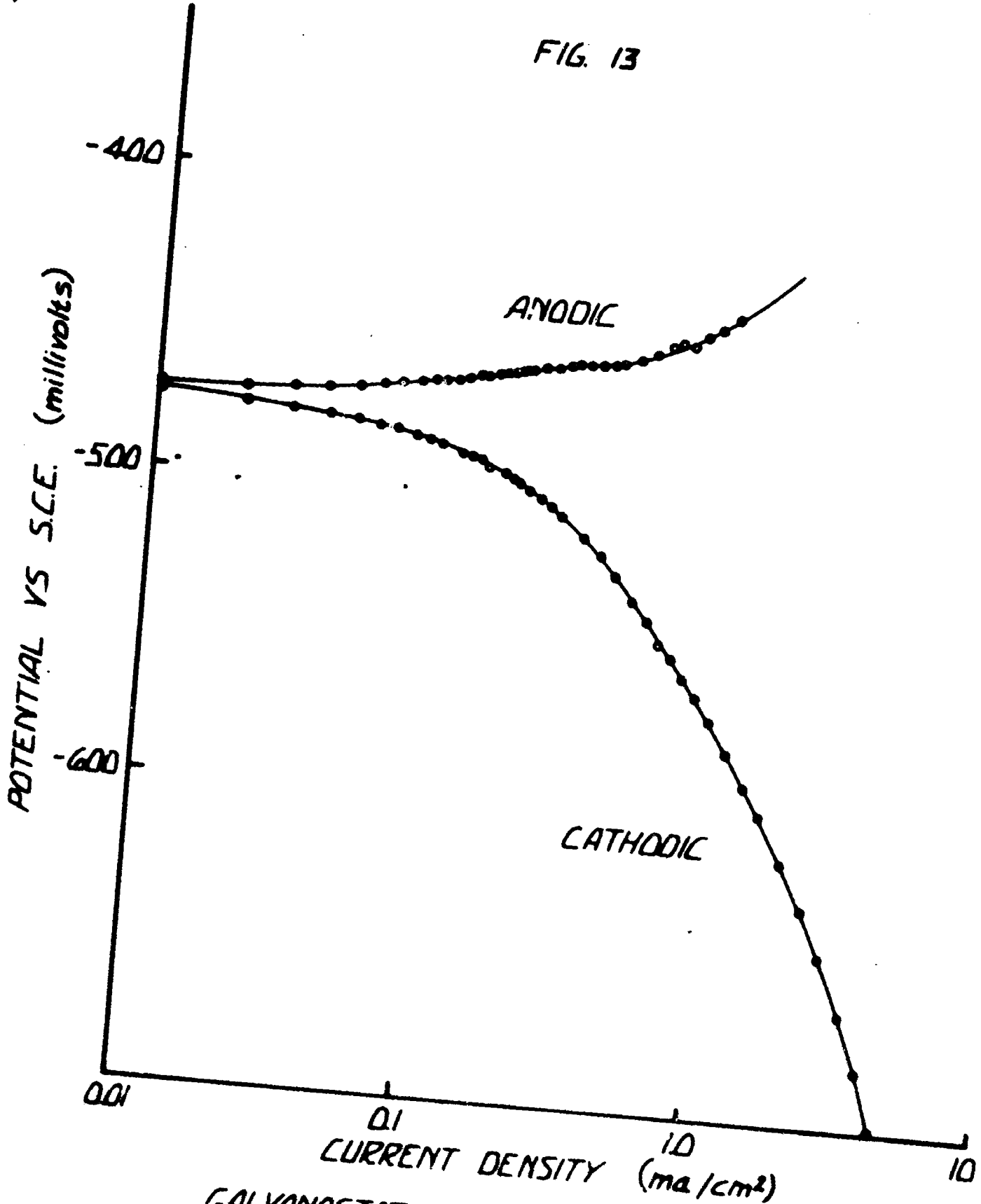
GALVANOSTATIC POLARIZATION CURVES  
FOR ARMCO IRON IN DEAERATED H<sub>2</sub>SO<sub>4</sub>

FIG. 12



GALVANOSTATIC POLARIZATION CURVES  
FOR ARMCO IRON IN pH 1 DEAERATED H<sub>2</sub>SO<sub>4</sub>

FIG. 13



GALVANOSTATIC POLARIZATION CURVES  
FOR ARMCO IRON IN 1N AERATED H<sub>2</sub>SO<sub>4</sub>

F1

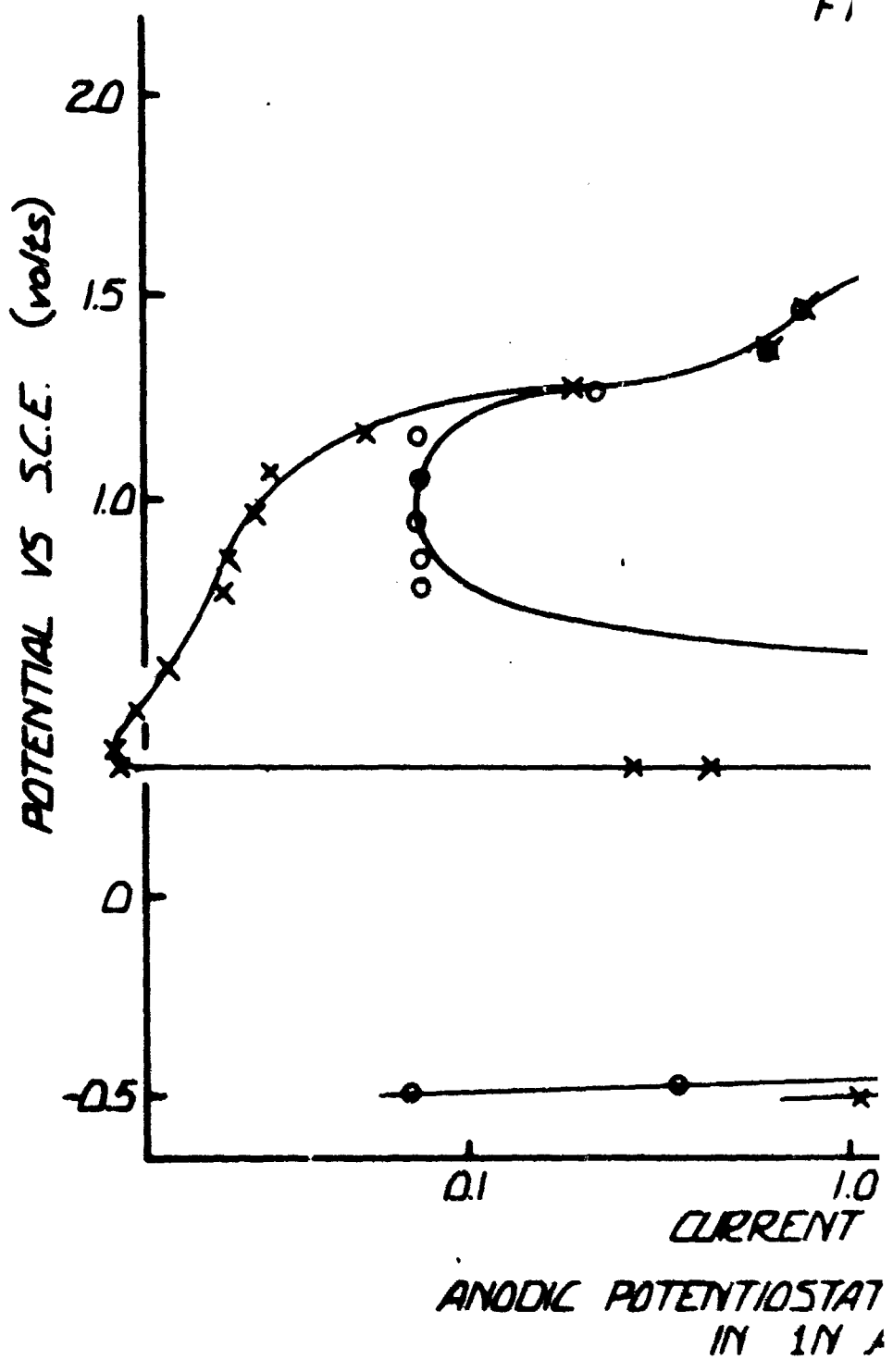
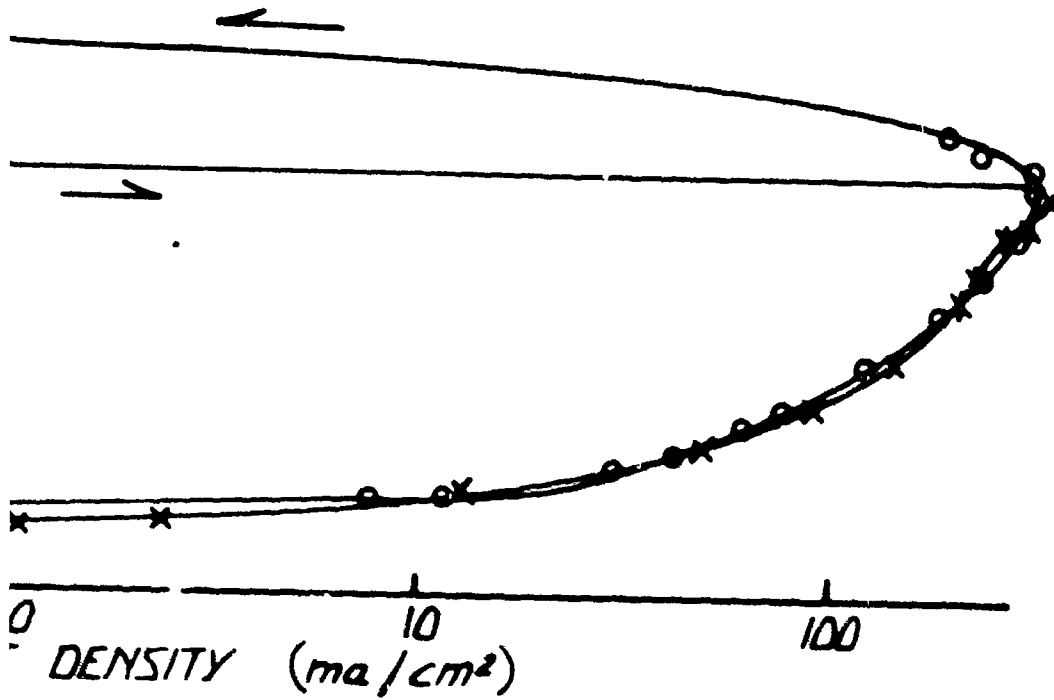
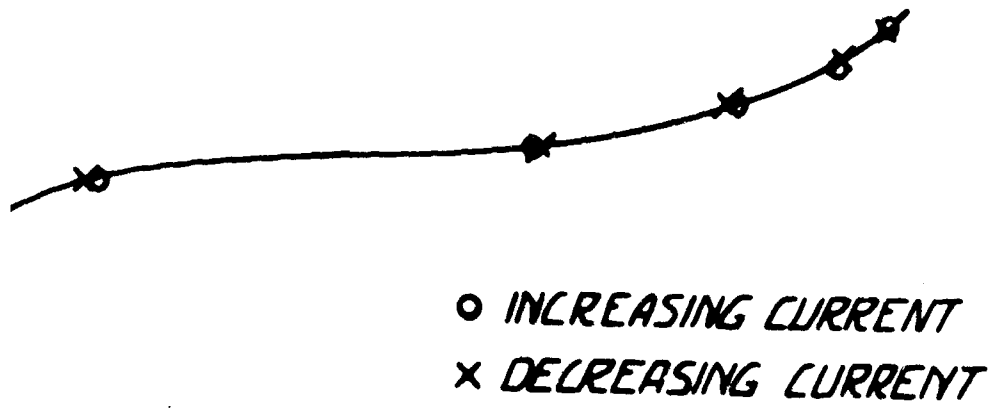
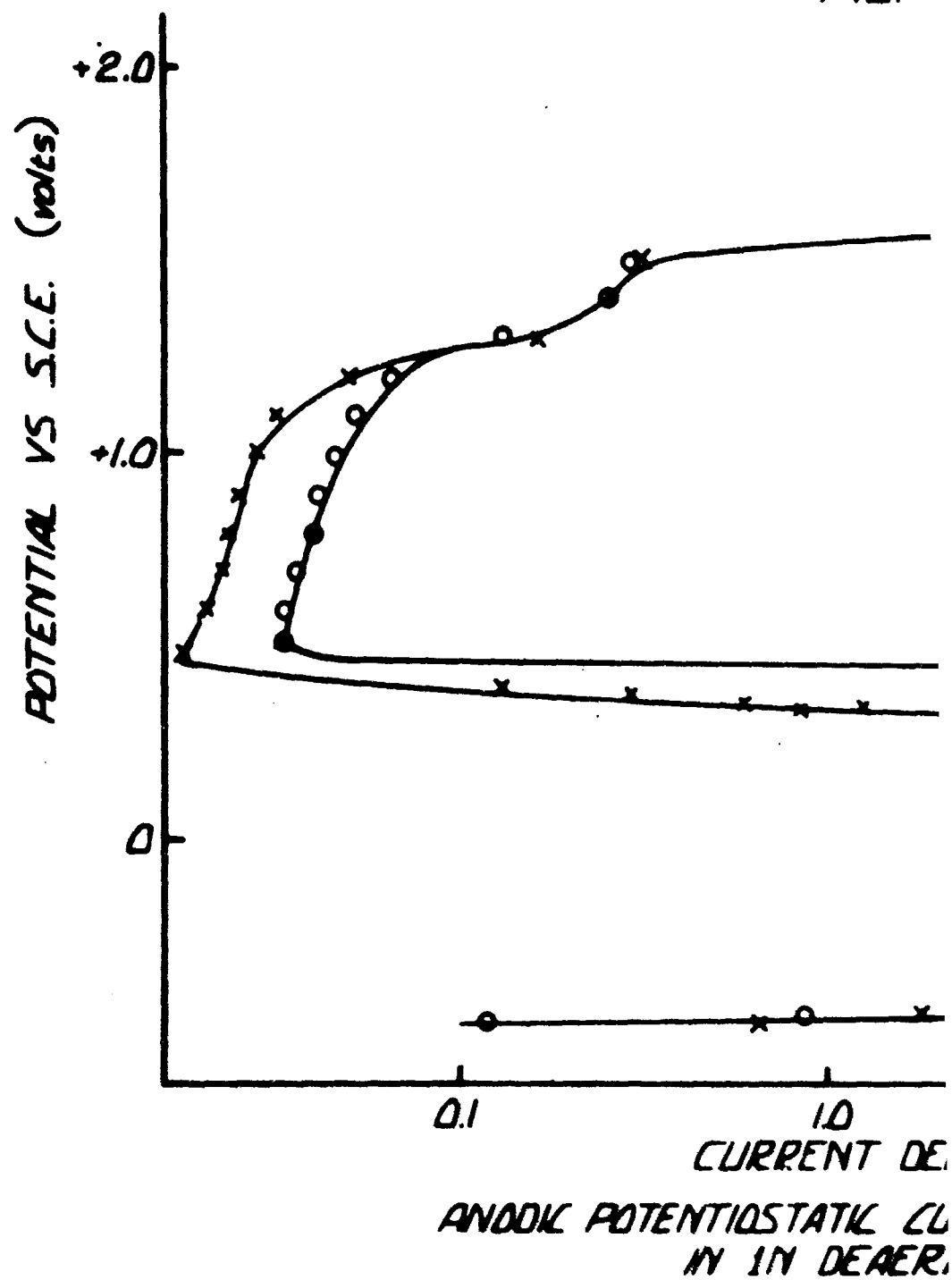


FIG. 14



VOLTAIC CURVE FOR ARMCO IRON  
IN AERATED H<sub>2</sub>SO<sub>4</sub>

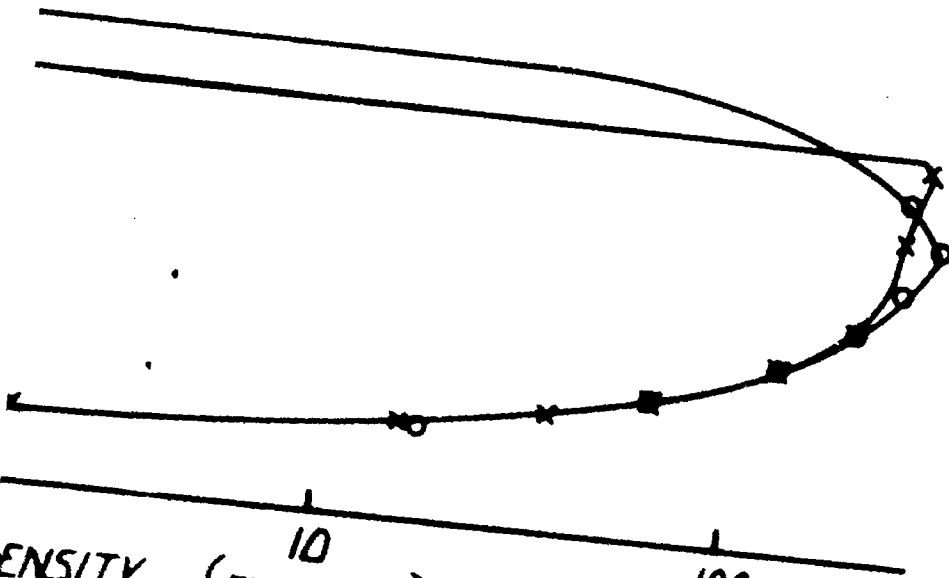
FIG.



15



o INCREASING CURRENT  
x DECREASING CURRENT



DENSITY (mA cm<sup>2</sup>)

10

100

CURVE FOR ARMCO IRON  
IN 1N H<sub>2</sub>SO<sub>4</sub>